Journal Name

ARTICLE TYPE

Supplementary material to:

The effect of alcohols as third component on diffusion in mixtures of aromatics and ketones

Tatjana Janzen[a], Yuri Gaponenko[b], Aliaksandr Mialdun[b], Gabriela Guevara-Carrion[a], Jadran Vrabec*[a], and Valentina Shevtsova*[b]

A Experimental method

The Taylor dispersion technique was used for measurements of binary and ternary diffusion coefficients. In its mathematical model, it is assumed that a homogeneous liquid mixture flows through a long, isothermal and straight tube of length L with a uniform, circular cross-section of radius R_0, having impermeable walls. The mixture is flowing in a slow, laminar manner with the mean velocity u. An injected narrow concentration pulse is dispersed due to the combined influence of the axial convection and molecular diffusion in radial direction. Further assumptions imply that diffusion coefficients are constant, which is valid if the concentration gradient is small, and no volume change occurs upon mixing. To satisfy the theoretical assumptions, Taylor dispersion experiments were carried out in capillaries with a small diameter. A Teflon (PTFE) tube of length $L=(29.839\pm0.001)$ m with a circular cross-section radius $R_0=374\,\mu$m was used. The capillary was coiled around a grooved aluminum cylinder with a diameter of 30 cm and was placed in a temperature-regulated air bath. A HPLC analytical pump (Knauer S1000) with active pulsation damping was used to push the carrier solution through the dispersion tube. The utilized Knauer Smartline RI Detector 2300 ($\lambda=950$ nm) is suited for recording small concentration variations with its differential sensitive refractometer. To prevent bubbles from disturbing the flow, the SYSTEC degassing module was installed and connected in-line before the pump. The flow rate during the measurements was 0.08 mL/min. Zero dead volume fittings were used to connect the capillary with the six port injection valve with injection volume $\Delta V=20\,\mu$L. The RI detector and the dispersion tube were kept in the same air bath at a constant temperature of 298 ± 0.2 K. The detector was connected to a computer for digital data acquisition using the Clarity Software by DataApex.

[a] *Thermodynamics and Energy Technology, University of Paderborn, Warburger Str. 100, D-33098 Paderborn, Germany. E-Mail: jadran.vrabec@upb.de*
[b] *Microgravity Research Center, Université Libre de Bruxelles, CP–165/62, Av. F.D. Roosevelt, 50, B–1050 Brussels, Belgium. E-mail: vshev@ulb.ac.be*

The diffusion equation for each component can then be written in the form[1,2]

$$\frac{\partial C_i}{\partial t} = \sum_{j=1}^{2} D_{ij}\left(\frac{\partial^2 C_j}{\partial z^2} + \frac{\partial^2 C_j}{\partial r^2} + \frac{1}{r}\frac{\partial C_j}{\partial r}\right) - u\left[1 - 2\left(\frac{r}{R_0}\right)^2\right]\frac{\partial C_i}{\partial z} \quad (i,j = 1,2), \tag{1}$$

where t is the time; r and z are the radial and axial coordinates, respectively.

In order to obtain an analytical solution of equation (1), an additional assumption is introduced: the axial transport by diffusion is small $\partial^2 C_j/\partial z^2 \ll \partial^2 C_j/\partial r^2 + r^{-1}\partial C_j/\partial r$, and can be neglected. Under these assumptions, the solution for the radially averaged concentrations of the injected samples can be found in an analytical form[2].

For a practical implementation, the concentration in the solution of equation (1) is replaced with the output signal $V(t)$ of a differential refractive index detector. Concentration differences ΔC_i between the injected sample and the carrier solution must be sufficiently small to ensure that the changes of the detector signal $V(t)$ are proportional to the changes of the concentration across the dispersion profiles

$$V(t) = \sum_{k=0}^{k=K} V_k t^k + R_1[C_1(t) - C_{10}] + R_2[C_2(t) - C_{20}], \tag{2}$$

where C_{i0} are the concentrations in the carrier solution, V_k are adjustable parameters of a baseline and $R_1 = (\partial V/\partial C_1)_{C_2}$ and $R_2 = (\partial V/\partial C_2)_{C_1}$ is the so-called "detector sensitivity".

Following Leaist[3], the analytical solution of equation (1) for a ternary mixture can be written as

$$V(t) = \sum_{k=0}^{k=K} V_k t^k + \Delta V_{\max}\sqrt{\frac{t_R}{t}}\left[W_1 \exp(-\hat{D}_1\eta) + (1 - W_1)\exp(-\hat{D}_2\eta)\right], \tag{3}$$

where $\eta = 12(t - t_R)^2/R_0^2 t$, $t_R = L/u$ is the retention time and $\hat{D}_i$ are the eigenvalues of the matrix of diffusion coefficients

$$\hat{D}_{1,2} = \frac{1}{2}\left(D_{11} + D_{22} \pm \sqrt{(D_{11} - D_{22})^2 + 4D_{12}D_{21}}\right). \tag{4}$$

The normalized weight W_1 is defined as

$$W_1 = \frac{(a + b\alpha)\sqrt{\hat{D}_2}}{(a + b\alpha)\sqrt{\hat{D}_1} + (1 - a - b\alpha)\sqrt{\hat{D}_2}}, \tag{5}$$

where the parameters a, b and α are

$$a = \frac{D_{11} - \hat{D}_1 - D_{12}S_R}{\hat{D}_2 - \hat{D}_1}, \tag{6}$$

$$b = \frac{D_{22} - D_{11} - D_{21}/S_R + D_{12}S_R}{\hat{D}_2 - \hat{D}_1}, \tag{7}$$

$$\alpha = \frac{\Delta C_1}{\Delta C_1 + \Delta C_2/S_R}. \tag{8}$$

Therein, $S_R = R_1/R_2$ is the optical sensitivity coefficient, which can be determined either by measuring the refractive indices of mixtures or by the relative ratio of the peak areas[4,5]. The basic tests and validation of the experimental set-up with binary and ternary mixtures were presented previously[4,6].

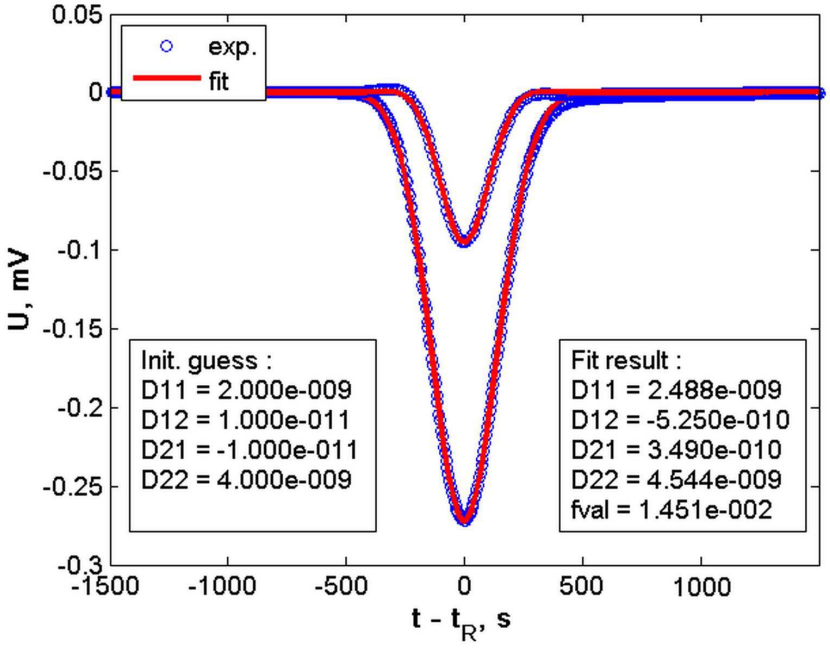

Fig. 1: Experimental Taylor dispersion peaks (symbols) for two different injections and fitting curves for the ternary mixture benzene + acetone + methanol with a composition (0.33, 0.57, 0.10) mol mol^{-1}.

The diffusion coefficients are obtained from the parameters of equation (3) that fit the experimental peaks. Instead of directly fitting D_{11}, D_{12}, D_{21} and D_{22}, we have used the parameters a, b and two eigenvalues. In order to determine four diffusion coefficients, two or more dispersion profiles have to be fitted simultaneously. A fit example of two peaks is shown in Figure 1 for the mixture benzene + acetone + methanol with a composition (0.33, 0.57, 0.10) mol mol^{-1}.

The diffusion coefficient matrix obtained experimentally from the Taylor dispersion technique provides coefficients in the volume reference frame, which have to be be transformed into the molar reference frame for comparison with molecular simulation data.

A.1 Fick diffusive flux equations in different reference frames

Molar fluxes in the volume reference frame ($u^v = \sum \phi_i u_i$) are

$$\begin{aligned} J_1^v &= x_1 \rho (u_1 - u^v) = -D_{11}^v \nabla C_1 - D_{12}^v \nabla C_2 \,, \\ J_2^v &= x_2 \rho (u_2 - u^v) = -D_{21}^v \nabla C_1 - D_{22}^v \nabla C_2 \,, \end{aligned} \tag{9}$$

and in the molar reference frame ($u = \sum x_i u_i$) they are

$$\begin{aligned} J_1 &= x_1 \rho (u_1 - u) = -\rho D_{11} \nabla x_1 - \rho D_{12} \nabla x_2 \,, \\ J_2 &= x_2 \rho (u_2 - u) = -\rho D_{21} \nabla x_1 - \rho D_{22} \nabla x_2 \,, \end{aligned} \tag{10}$$

with molar density ρ.

Transformation of Fick coefficients between volume and molar reference frames[7]

$$\begin{aligned} \mathbf{D}^{\mathrm{v}} &= \mathbf{B}^{Vu} \times \mathbf{D} \times \mathbf{B}^{uV}\,, \\ B_{ik}^{Vu} &= \delta_{ik} - x_i(v_k - v_n)/v\,, \\ B_{ik}^{uV} &= \delta_{ik} - x_i(1 - v_k/v_n) \quad \text{with} \quad [B^{Vu}]^{-1} = [B^{uV}]\,. \end{aligned} \tag{11}$$

The transformation of the experimental data from the volume to the molar reference frame (D_{ij}^{v} to D_{ij}) was done on the basis of pure component volumes. Carrying out dedicated density measurements, it was found that that the differences between partial molar volumes, which have to be used for a strict transformation, and pure component volumes are negligible.

B Computational details and model parameters

B.1 Simulation details

All molecular dynamics (MD) simulations were carried out with the program *ms*2[8–10]. A cubic volume was assumed with periodic boundary conditions containing 4000 molecules. Intermolecular interactions were explicitly evaluated within a cutoff radius of 17.5 Å, considering the LJ long-range corrections beyond the cutoff radius with the angle-averaging method of Lustig[11] and the long-range electrostatic interactions by means of the reaction field method[12].

The simulations were conducted in the canonic (NVT) ensemble, while the temperature was controlled by velocity scaling[13]. The simulations were first equilibrated over 4×10^5 time steps followed by production runs of 4 to 5 $\times 10^7$ time steps. Newton's equations of motion were solved with a fifth-order Gear predictor-corrector numerical integrator and an integration time step of $\sim$ 1.02 fs. The phenomenological diffusion coefficients were calculated by averaging up to 4.9×10^5 independent time origins of the correlation functions with a sampling length of 20.5 ps for the individual correlation functions.

B.2 Flux equations

Molar fluxes according to irreversible thermodynamics in the mass reference frame ($u^m = \sum w_i u_i$)

$$\begin{aligned} J_1^m/\rho &= x_1(u_1 - u^m) = -\frac{1}{RT}\Lambda_{11}\nabla\mu_1 - \frac{1}{RT}\Lambda_{12}\nabla\mu_2 - \frac{1}{RT}\Lambda_{13}\nabla\mu_3\,, \\ J_2^m/\rho &= x_2(u_2 - u^m) = -\frac{1}{RT}\Lambda_{21}\nabla\mu_1 - \frac{1}{RT}\Lambda_{22}\nabla\mu_2 - \frac{1}{RT}\Lambda_{23}\nabla\mu_3\,, \\ J_3^m/\rho &= x_3(u_3 - u^m) = -\frac{1}{RT}\Lambda_{31}\nabla\mu_1 - \frac{1}{RT}\Lambda_{32}\nabla\mu_2 - \frac{1}{RT}\Lambda_{33}\nabla\mu_3\,. \end{aligned} \tag{12}$$

In equilibrium MD simulation, the mass averaged velocity u^m is typically set to zero when the net momentum is set to zero.

Coefficients obtained by MD simulation with the Green-Kubo formalism[14] are

$$\Lambda_{ij} = \frac{1}{3N}\int_0^\infty \left\langle \sum_{k=1}^{N_i} \mathbf{v}_i^k(0) \cdot \sum_{l=1}^{N_j} \mathbf{v}_j^l(t) \right\rangle \mathrm{d}t\,, \tag{13}$$

where N is the total number of molecules. The coefficients are constrained by $\Lambda_{ij} = \Lambda_{ji}$ and $\sum M_i \Lambda_{ij} = 0$.

Because there are only two independent fluxes and driving forces in a ternary mixture, the equations can be transformed to the following form in the molar reference frame

$$\begin{aligned} J_1/\rho &= -\Delta_{11}\frac{x_1}{RT}\nabla\mu_1 - \Delta_{12}\frac{x_2}{RT}\nabla\mu_2\,, \\ J_2/\rho &= -\Delta_{21}\frac{x_1}{RT}\nabla\mu_1 - \Delta_{22}\frac{x_2}{RT}\nabla\mu_2\,. \end{aligned} \tag{14}$$

Transformation of the phenomenological coefficients is

$$\begin{aligned} \Delta_{11} &= (1-x_1)\left(\frac{\Lambda_{11}}{x_1} - \frac{\Lambda_{13}}{x_3}\right) - x_1\left(\frac{\Lambda_{21}}{x_1} - \frac{\Lambda_{23}}{x_3} + \frac{\Lambda_{31}}{x_1} - \frac{\Lambda_{33}}{x_3}\right), \\ \Delta_{12} &= (1-x_1)\left(\frac{\Lambda_{12}}{x_2} - \frac{\Lambda_{13}}{x_3}\right) - x_1\left(\frac{\Lambda_{22}}{x_2} - \frac{\Lambda_{23}}{x_3} + \frac{\Lambda_{32}}{x_2} - \frac{\Lambda_{33}}{x_3}\right), \\ \Delta_{21} &= (1-x_2)\left(\frac{\Lambda_{21}}{x_1} - \frac{\Lambda_{23}}{x_3}\right) - x_2\left(\frac{\Lambda_{11}}{x_1} - \frac{\Lambda_{13}}{x_3} + \frac{\Lambda_{31}}{x_1} - \frac{\Lambda_{33}}{x_3}\right), \\ \Delta_{22} &= (1-x_2)\left(\frac{\Lambda_{22}}{x_2} - \frac{\Lambda_{23}}{x_3}\right) - x_2\left(\frac{\Lambda_{12}}{x_2} - \frac{\Lambda_{13}}{x_3} + \frac{\Lambda_{32}}{x_2} - \frac{\Lambda_{33}}{x_3}\right). \end{aligned} \tag{15}$$

Transformation to the Fick diffusion coefficients in the molar reference frame is

$$\mathbf{D} = \boldsymbol{\Delta} \times \boldsymbol{\Gamma}. \tag{16}$$

Thermodynamic factor matrix for the transformation between different driving forces is[15]

$$\frac{x_i}{RT}\nabla\mu_i = \sum_{j=1}^{n-1}\Gamma_{ij}\nabla x_j\,, \tag{17}$$

$$\begin{aligned} \Gamma_{ij} &= \frac{x_i}{RT}\frac{\partial\mu_i}{\partial x_j}\Big|_{T,p,\Sigma} = \frac{x_i}{RT}\frac{RT\,\partial\ln(x_i\gamma_i)}{\partial x_j}\Big|_{T,p,\Sigma} \\ &= \delta_{ij} + x_i\frac{\partial\ln\gamma_i}{\partial x_j}\Big|_{T,p,\Sigma} = \delta_{ij} + x_i\left(\frac{\partial\ln\gamma_i}{\partial x_j}\Big|_{T,p,x_{k\neq j}} - \frac{\partial\ln\gamma_i}{\partial x_n}\Big|_{T,p,x_{k\neq n}}\right). \end{aligned} \tag{18}$$

Table 1: Wilson g^{E} model parameters.

component	v_i cm^3 mol^{-1}	comp. 1	comp. 2	$\Delta\lambda_{ij}/R$ K	$\Delta\lambda_{ji}/R$ K
acetone	73.876	benzene	acetone	-45.574	198.045
benzene	89.711	benzene	methanol	85.839	1030.889
methanol	40.749	acetone	methanol	-72.439	309.734
ethanol	58.372	benzene	ethanol	72.021	871.861
2-propanol	77.034	acetone	ethanol	12.531	196.077
		benzene	2-propanol	147.759	488.692
		acetone	2-propanol	131.842	116.611

B.3 Wilson excess Gibbs energy model

The elements of the thermodynamic factor matrix can be calculated by the Wilson excess Gibbs energy (g^{E}) model from[15]

$$\begin{aligned} \Gamma_{ij} &= \delta_{ij} + x_i(Q_{ij} - Q_{in}), \\ Q_{ij} &= -\frac{A_{ij}}{S_i} - \frac{A_{ji}}{S_j} + \sum_{k=1}^{n} \frac{x_k A_{ki}}{S_k}, \\ S_i &= \sum_{j=1}^{n} x_j A_{ij}\ , \quad A_{ij} = \frac{v_j}{v_i} \exp\left(-\frac{\Delta\lambda_{ij}}{RT}\right), \end{aligned} \tag{19}$$

with the molar volumes of the pure components v_i and the binary Wilson parameters λ_{ij} listed in Table 1.

B.4 Molecular force fields

Molecular force field model parameters from previous work: benzene[16], acetone[17], methanol[18], ethanol[19]. New force field parameters for 2-propanol[20]. All parameters listed in Table 2.

Table 2: Lennard-Jones parameters (σ and ε) and electrostatic parameters (quadrupole Q, dipole D or point charge q) as well as spatial site positions of the molecular force field models used in this work.

site	x Å	y Å	z Å	M a.u.	σ Å	ε/k_B K	Q DÅ	D D	q e
benzene									
CH	0	0	0	13.0	3.446	70.019	-1.0435	-	-
CH	-1.6303	0	0	13.0	3.446	70.019	-1.0435	-	-
CH	-2.4455	1.4119	0	13.0	3.446	70.019	-1.0435	-	-
CH	-1.6303	2.8238	0	13.0	3.446	70.019	-1.0435	-	-
CH	0	2.8238	0	13.0	3.446	70.019	-1.0435	-	-
CH	0.8152	1.4119	0	13.0	3.446	70.019	-1.0435	-	-
acetone									
C	0	0	0	12.0	2.9307	9.8216	-	3.4448	-
O	0	1.2095	0	16.0	3.3704	106.9873	-	-	-
CH_3	0	-0.8031	1.2853	15.0	3.6225	111.9795	-	-	-
CH_3	0	-0.8031	-1.2853	15.0	3.6225	111.9795	-	-	-
	0	-0.8031	0	-	-	-	-0.8031	-	-
methanol									
CH_3	0.7660	0.0134	0	15.034	3.7543	120.592	-	-	0.24746
O	-0.6565	-0.0640	0	16.0	3.0300	87.879	-	-	-0.67874
H	-1.0050	0.8146	0	1.008	-	-	-	-	0.43128
ethanol									
CH_3	-1.471	-0.338	0	15	3.6072	120.15	-	-	-
CH_2	0.093	0.883	0	14	3.4612	86.291	-	-	0.25560
O	1.172	-0.451	0	16	3.1496	85.053	-	-	-0.69711
H	2.049	-0.086	0	1	-	-	-	-	0.44151
2-propanol									
CH_3	-1.1090	2.1279	-1.2649	15.0355	3.8656	103.590	-	-	-
CH_3	-3.0811	1.1352	0.0766	15.0355	3.8656	103.590	-	-	-
CH	-1.5519	1.3442	0	13.0195	3.2383	20.200	-	-	0.30974
O	-0.9689	0	0	15.9995	3.1538	85.904	-	-	-0.74720
H	0	0	0	1.008	-	-	-	-	0.43746

References

1 A. Alizadeh, C. A. Nieto de Castro and W. A. Wakeham, *International Journal of Thermophysics*, 1980, **1**, 243–284.

2 W. E. Price, *J. Chem. Soc., Faraday Trans. 1*, 1988, **84**, 2431–2439.

3 D. G. Leaist, *J. Chem. Soc., Faraday Trans.*, 1991, **87**, 597–601.

4 J. C. Legros, Y. Gaponenko, A. Mialdun, T. Triller, A. Hammon, C. Bauer, W. Kohler and V. Shevtsova, *Phys. Chem. Chem. Phys.*, 2015, **17**, 27713–27725.

5 V. Sechenyh, J. C. Legros, A. Mialdun, J. M. Ortiz de Zárate and V. Shevtsova, *J. Phys. Chem. B*, 2016, **120**, 535–548.

6 G. Guevara-Carrion, Y. Gaponenko, T. Janzen, J. Vrabec and V. Shevtsova, *J. Phys. Chem. B*, 2016, **120**, 12193–12210.

7 R. Taylor and R. Krishna, *Multicomponent Mass Transfer*, John Wiley & Sons, New York, 1993.

8 S. Deublein, B. Eckl, J. Stoll, S. V. Lishchuk, G. Guevara-Carrion, C. W. Glass, T. Merker, M. Bernreuther, H. Hasse and J. Vrabec, *Comput. Phys. Commun.*, 2011, **182**, 2350–2367.

9 C. W. Glass, S. Reiser, G. Rutkai, S. Deublein, A. Köster, G. Guevara-Carrion, A. Wafai, M. Horsch, M. Bernreuther, T. Windmann, H. Hasse and J. Vrabec, *Comp. Phys. Commun.*, 2014, **185**, 3302–3306.

10 G. Rutkai, A. Köster, G. Guevara-Carrion, T. Janzen, M. Schappals, C. W. Glass, M. Bernreuther, A. Wafai, S. Stephan, M. Kohns, S. Reiser, S. Deublein, M. Horsch, H. Hasse and J. Vrabec, *Comp. Phys. Commun.*, 2017, **221**, 343 – 351.

11 R. Lustig, *Mol. Phys.*, 1988, **65**, 175–179.

12 J. A. Barker and R. O. Watts, *Mol. Phys.*, 1973, **26**, 789–792.

13 M. P. Allen and D. J. Tildesley, *Computer Simulation of Liquids*, Clarendon Press, Oxford, 1987.

14 R. Krishna and J. M. van Baten, *Ind. Eng. Chem. Res.*, 2005, **44**, 6939–6947.

15 R. Taylor and H. A. Kooijman, *Chem. Eng. Comm.*, 1991, **102**, 87–106.

16 G. Guevara-Carrion, T. Janzen, Y. M. Muñoz-Muñoz and J. Vrabec, *J. Chem. Phys.*, 2016, **144**, 124501.

17 T. Windmann, M. Linnemann and J. Vrabec, *J. Chem. Eng. Data*, 2014, **59**, 28–38.

18 T. Schnabel, A. Srivastava, J. Vrabec and H. Hasse, *J. Phys. Chem. B*, 2007, **111**, 9871–9878.

19 T. Schnabel, J. Vrabec and H. Hasse, *Fluid Phase Equilib.*, 2005, **233**, 134–143.

20 Y. M. Muñoz-Muñoz, G. Guevara-Carrion and J. Vrabec, *unpublished manuscript*, 2018.